MODELLING OF NON-IDEAL PARTICLES AND DROPLETS IN FLUID-SOLID AND FLUID-FLUID-SOLID PROCESSES

Tapio Salmi[a*], Vincenzo Russo[b], Johan Wärnå[a,] Dmitry Yu. Murzin[a], Henrik Grénman[a]

a Åbo Akademi, PCC/Chemical Engineering, –Turku/Åbo, FI 20500, Finland
b Università di Napoli 'Federico II', – Napoli, IT 80126, Italy

Abstract

A generalized mathematical model was developed for non-ideal reactive solid particles and liquid droplets. The model takes into account non-ideal geometric effects, such as cracks, craters, pores and non-spherical forms of reactive solids and droplets. The model was successfully applied to several industrially very relevant cases, such as leaching of zinc ores, reactions of limestone with sulphuric acid and synthesis of sodium hydride from melt sodium droplets.

Keywords

Fluid-Solid and Fluid-Fluid Processes, Non-Ideal Geometry, Kinetics, Mass Transfer

*To whom all correspondence should be addressed

Introduction

Solid-liquid and solid-liquid-liquid reactions have wide applications in industrial scale, from mining to the production of fine chemicals, food ingredients and pharmaceuticals. The classical models are very much based on the assumption of ideal particle geometry, i.e. slab, infinitely long cylinder and perfect sphere. Mathematical expressions are available in textbooks for shrinking particle, product layer and grain models (Levenspiel 1990, Salmi et al. 2011).

The assumption of an ideal geometric form is a serious limitation contradicting many experimental observations. Microscopic studies reveal the real particle morphology, as illustrated by Figure 1, where some scanning electron microscopic images of reactive particles are shown. Real particles can have an irregular form, they can consist of agglomerates and cracks and craters appear on the outer surface during the reaction.

In laboratory-scale experiments, high stirring rates are applied which causes turbulence around the particles, and the diffusion resistance in the film around the particle is diminished. High stirring rates cannot always be applied in large-scale reactors, which implies that the film resistance around particles and droplets affects the overall rate of the process. In case of shrinking particles, the film thickness diminishes as the reaction proceeds: the role of the film resistance declines for very small particles.

We developed a generalized model which takes into account the non-idealities of solid particles and liquid droplets as well as the gradual change of the film resistance during the progress of the reaction. The model can be applied to all particle and droplet morphologies, from perfect spheres to completely porous particles.
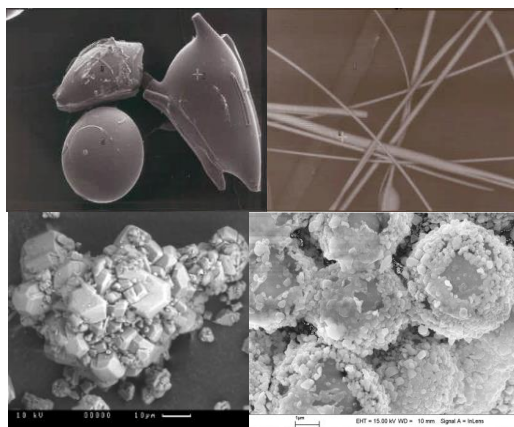

Figure 1. SEM images of some real reactive solid particles (upper: mineral wool, lower: zinc sphalerite).

Modelling principles

The core idea of the model is the generalization of the particle geometry by introducing the shape factor $a=s+1 =A_P/V_P R$, where A_P and V_P are the outer surface and the volume of the particle and R is the characteristic dimension of the particle (R=radius of sphere or cylinder, half-thickness of slab). For a non-porous, ideal sphere, $s+1=3$, but as defects appear on the surface or the particle

is porous, the outer surface (A_P) increases and the shape factor gets values higher than 3. The rate is proportional to the available area, A_P, which is proportional to the amount of substance $n_i^{s/(s+1)}$. For particles with pores or defects and for non-ideal droplets, s can become high and the effective reaction order approaches 1.

A stirred batch reactor was considered in the modelling. The mass balance equation for a solid particle or a dispersed bubble has the general form

$$\frac{dn_j}{dt} = -r\frac{(s+1)M}{\rho R_0} n_{0j}^{1/(s+1)} n_j^{s/(s+1)}$$

where n_j denotes the amount of substance (in mol) in the suspension at time t; n_{0j}= initial amount of the substance, s is the shape factor of the particle or the droplet, R_0=initial particle or droplet radius, M=molar mass, ρ=density. The rate expression (r) depends on the specific reaction mechanism. The concentration of the liquid-phase component (included in r) at the particle or droplet surface is affected by the mass transfer in the film surrounding the particle or the droplet. By applying the generally accepted correlation (Temkin 1977, Wakao 1984) which relates the Sherwood number with the Reynolds and Schmidt numbers, the dimensionless film thickness (δ/R_0) can be expressed as

$$\delta/R_0 = \left(\frac{n_j}{n_{0j}}\right)^{1/(s+1)} \left(1 + \alpha\left(\frac{n_j}{n_{0j}}\right)^{2/(3(s+1))}\right)^{-1}$$

where α is a dimensionless number, which is 0 for silent conditions and increases with an increasing mixing rate. The film thickness is used to calculate the mass transfer coefficient for the liquid film surrounding the particle or the droplet.

The differential-algebraic (DAE) model was solved numerically by a stiff ODE solver during the minimization of the objective function in the parameter estimation. The numerical values of the kinetic parameters were determined in the estimation. The gPROMS Model Builder v.4 software was used in most cases.

An illustration example, the synthesis of NaH(s) from liquid droplets of Na(l, finely dispersed in mineral oil) by hydrogenation is illustrated in Figure 2. The model was able to predict the conversion of Na very well at different stirring rates in a tailored test reactor. A further proof of the model validity was obtained with linearized test plots (Levenspiel 1990, Salmi et al. 2011) presented in Figure 3.

Conclusions

The proposed general model was successfully applied to several cases, such as leaching of zinc ores, reactions of limestone with sulphuric acid and synthesis of sodium hydride from melt sodium droplets. An extensive series of experiments was carried out in isothermal laboratory-scale reactors (100-400 mL) under atmospheric pressure.
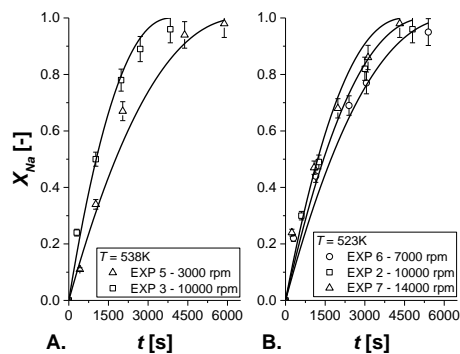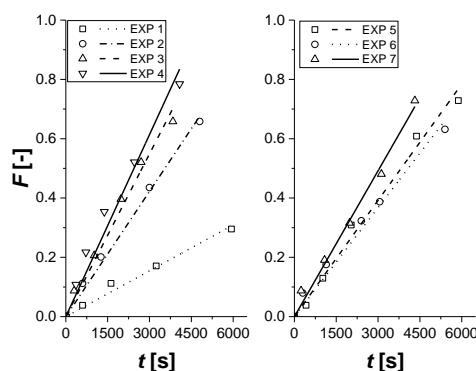
Figure 2. Effect of the stirring rate on the sodium conversion in the synthesis of NaH at: A. 538K; B. 523K. The continuous lines represent the model predictions.

$$F = 1-(1-X)^{1/(s+1)} = t/\tau$$

Figure 3. F function test plot vs the reaction time for each experiment in the synthesis of NaH. Calculated values were obtained by linear fit to the experimental data.

References
gPROMS Model Builder, Process Systems Enterprise (https://www.psenterprise.com/) (11/06/2018)

Levenspiel, O. (1990). *Chemical Reaction Engineering*, 3rd ed. Wiley, New York.

Salmi, T., Mikkola, J.-P., Wärnå, J. (2011). *Chemical Reaction Engineering and Reactor Technology*, CRC Press Taylor & Francis Group Boca Raton Fl.

Temkin, M.I. (1977). Transfer of dissolved matter between a turbulently moving liquid and particles suspended in it, *Kinetika i Kataliz, 18*, 493-496.

Wakao, N. (1984). *Recent Analysis of Chemically Reacting Systems* (Ed. Doraiswamy, L.K.), Wiley Eastern, New Delhi